Transponder Satellite Payload Measurements: Uncertainty Review for Different Levels of Accessibility

Grigory Kuznetsov, *Member, AMTA*
Gennady Pinchuk, *Member, AMTA*
Cosme Culotta-López, *Member, AMTA*
Gil Yemini, *Member, AMTA*
Lior Shmidov
Orbit/FR Engineering Ltd. (MVG), Israel
grigory.kuznetsov@mvg-world.com

Andrea Giacomini, *Senior Member, AMTA*
Lars J. Foged, *Fellow, AMTA*
Microwave Vision Italy SRL (MVG), Italy
andrea.giacomini@mvg-world.com

***Abstract*—Transceiver satellites with a "bent-pipe" payload are commonly used in communication systems. Accuracy of measurement of their main End-to-End (E2E) parameters, such as Saturating Flux Density (SFD), Gain flatness (G/F), Equivalent Isotropic Radiated Power (EIRP) and Gain over Temperature (G/T) depends not only on the test setup, but also on the accessibility of different test points in the payload. In this work, we focus on the error budget for different accessibility levels when the payload is tested in Planar Near-Field (PNF).**

I. Introduction

The first satellite payloads were relatively simple, often consisting of a single antenna and basic transponder functionality. However, as communication demands grow, payloads become more sophisticated, incorporating multiple antennas, frequency converters, and complex signal processing. The emergence of the "bent-pipe" payload architecture provides a versatile solution [1]. By separating the uplink and downlink functions, it allows for independent optimization of each antenna's performance. The frequency-converting payload acts as a bridge, translating signals between the two frequency bands, offering flexibility in system design. System designers, however, face critical decisions regarding the integration of payload components. The choice of which points to make accessible during testing significantly impacts measurement accuracy, notably of End-to-End (E2E) and system-level parameters—such as Saturating Flux Density (SFD), Gain flatness (G/F), Equivalent Isotropic Radiated Power (EIRP), and Gain over Temperature (G/T).

In this paper, we analyze the uncertainties that arise during measurements of transceiver satellite payload. Depending on the choice of accessibility level, different test setups are available [2]–[4], with different measurement uncertainties.
For antenna measurement systems, there are several important points that define the possible test setups, accuracy, and measurement speed, namely:

- The antenna ports, either directly or through a test coupler.
- Frequency converter LO source, either taken from a coupler or injected from the test setup.

From there, there are several options:

- Full integration: no antenna access and no LO access in any way. This option usually requires using a Compact Range (CATR) [2], [5], as there is no phase information present. Near-field solutions are possible, but there are limitations that reduce accuracy.
- Both antenna couplers and LO source are accessible: Near-field setups are possible.
- Antenna accessible, but not LO: NF possible, with some limitations on payload parameter testing.
- LO source accessible, but not antennas: NF possible, with additional test hardware.

We focus on Planar Near-Field (PNF) setups, as both uplink and downlink antennas are usually very directive. From there, we elaborate on the estimation of the uncertainties of the following parameters: antenna gain, Gain over Temperature (G/T) [6], Equivalent isotropic radiated power (EIRP), Gain over Frequency (G/F, gain flatness) [7], [8]; with a discussion on how the accessibility level influences them.

This paper is organized as follows. In Section II, a typical transponder payload block diagram is presented and various test/access points are identified, and the different measurement scenarios are described in more detail. In Section III, the total measurement uncertainties are calculated. Section IV concludes the paper.

II. Payload Measurement Setups

A. Transponder Payload Overview

In Fig. 1, a typical "bent-pipe" payload ("transparent satellite") is presented. Access to the test couplers (if any) and LO generator(s) simplifies the design of the payload measurements. In the next Subsections, the different configurations are explained.

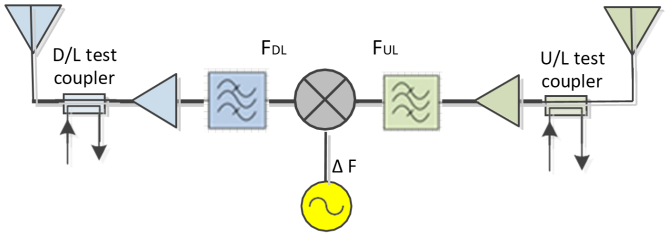

Fig. 1: Transponder payload block diagram

B. Full access

With full access to the couplers and the LO source, one can inject the signal from an external RF generator from the uplink coupler side (or into the uplink antenna directly through an NF probe). One option is to use an external frequency converter that replicates the internal converter to create a reference signal that is coherent with the signal transmitted by a downlink antenna.

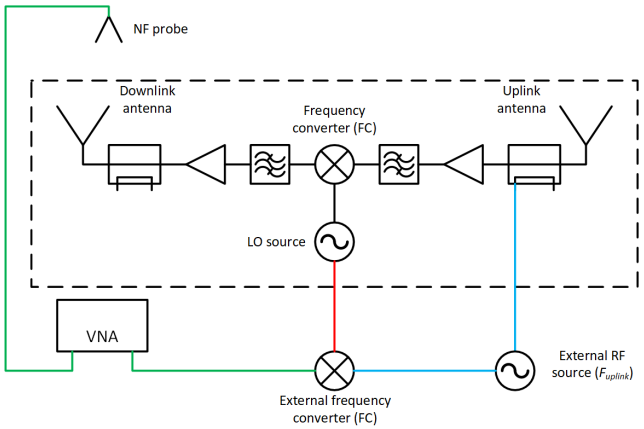

Fig. 2: Full payload access: downlink antenna measurements

This allows measuring pattern and EIRP of the downlink antenna directly, as shown, for example, in [7]. Uplink antenna pattern can be easily measured simply by connecting to the uplink coupler, but the G/T and saturating flux density require additional measurements on downlink side (from coupler or over-the-air through the probe). These measurements do not require phase information, so they can also be measured without LO access. This is discussed in the next subsection.

C. Antenna couplers only

As the patterns of antennas can be measured using couplers, here we will focus on end-to-end (E2E) payload parameters: EIRP, G/T, E2E gain over frequency (G/F), saturating flux density (SFD).

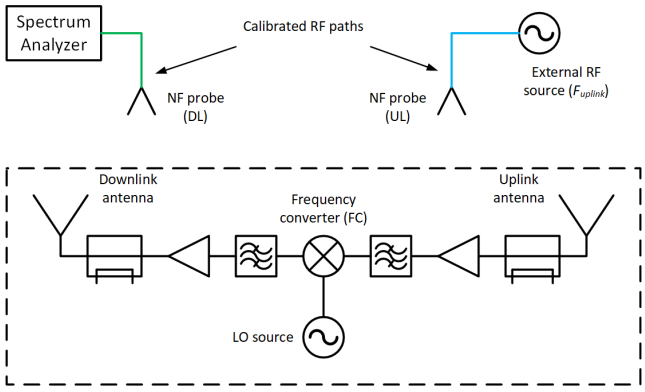

Fig. 3: No LO access: end-to-end parameters measurements

All of these parameters require measuring not only relative values (transmission coefficient between probe and AUT), but also absolute power values. Because of this, the uplink signal must be stable in output power, and all RF paths between probes and power source/power meter/spectrum analyzer should be calibrated. Any error in these calibrations is directly translated to power measurement uncertainties.

D. LO access only

With no access to the test couplers of antennas, even the pattern measurements in the near-field become a problem, and without these data, E2E parameters cannot be measured. And LO access can be organized in a number of ways:

- Direct output of LO through a coupler/divider.
- High-frequency LO is not available directly, but the output of a reference crystal oscillator (XO) is available.

The first option was shown above in section II-B. The second option requires either hardware up-conversion of XO output to get back the LO, or using a high-speed multi-channel RF digitizer (such as an oscilloscope) to capture both XO and RF signals (UL/DL) in the same timebase and downconvert the signals mathematically.

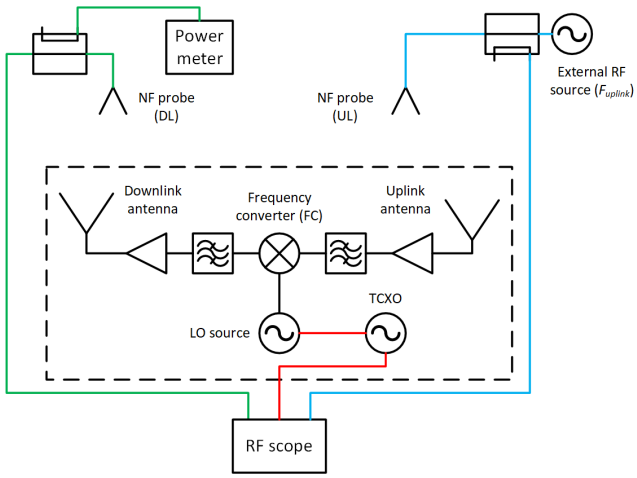

Fig. 4: Antenna and E2E measurements with XO as reference

This approach brings an additional error source to the measurements: as internal LO source most likely uses a phase-locked loop (PLL) generator, its phase noise differs from the phase noise of the restored LO. While the dynamic range of the system may seem high, additional phase errors will reduce the accuracy of pattern measurements. A uniformly distributed phase error of $\pm 10^\circ$ will cause an error of $-0.05\,\mathrm{dB}$ in gain (equivalent to $-45\,\mathrm{dB}$ noise), and $\pm 20^\circ$ error will cause $-0.18\,\mathrm{dB}$ of error. These errors are also directly translated into EIRP and G/T.

E. Fully integrated payload

As noted in the introduction, measurements of a fully integrated payload (without any mentioned test points) are possible in CATR, but near-field measurements become complicated. Tx (downlink) measurements are possible with the use of an additional static (non-moving) probe that senses the transmitted field and provides phase reference for the signal measured by the moving probe, as shown in the Figure 5.

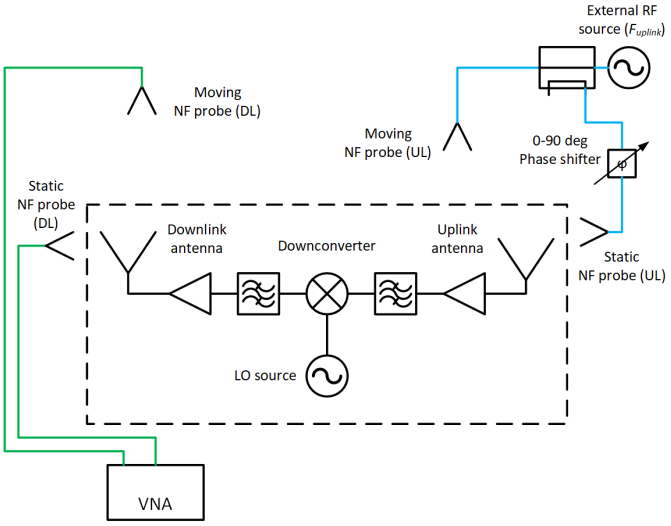

Fig. 5: Integrated payload measurement setup

Measurements of the Rx side (uplink) are more complicated, because there is no LO access, and phaseless methods are needed for this measurement. One of the methods of phase reconstruction is by using yet another static probe antenna to inject the signal into the DUT, but this channel must be able to switch phase between 0 and 90°. In this case, 4 amplitude-only measurements are required at each measurement point: moving probe signal only, static probe signal only, sum of moving and static(0° phase), sum of moving and static (90° phase).

If the phase introduced by a phase shifter is not exactly (90°, but differs by some $\Delta\phi$, then the error of $0...\Delta\phi$ is added to all measurements, and this error depends on the value of the measured phase. For high-gain antennas directed to the boresight (perpendicular to PNF measurement plane), phase of the measured field is usually almost constant, and the introduced error is also an almost a constant phase shift. However, for any off-boresight position of the measured beam a $\Delta\phi$ "ripple" in phase distribution will be added to the AUT field distribution. As an estimate, a 10° phase error will translate into about 0.035 dB gain error.

While this phase error is small and predictable, there is another source of measurement error in this scenario: a moving PNF probe reflects some of the field radiated by the static probe back into the antenna. As the static probe cannot be located in front of the AUT aperture (moving probe needs to see the aperture without obstruction), the coupling between static probe and AUT is low. But the reflections from the moving probe and its carrier axis are easily coupled to DUT, and they can easily become close in amplitude to the direct signal from the static probe. This error level can be higher than the the level of chamber absorber reflections (typically -50 dB) and can become one of the major limitations of measurement accuracy.

III. Uncertainty Calculation

Here we will review the commonly used formulas for E2E parameters calculated from NF measurements and how the uncertainties described above influence the final error budget. We will start with detailed analysis of uncertainties for EIRP measurements. For other parameters, we will make notes on error sources and their values, if they differ from the ones used in EIRP calculation.

A. EIRP

The formula for EIRP calculation is shown below, where M_{EIRP} is a mismatch factor, P_{pr} is a received power at the probe output measured at x_0, y_0 coordinates, $b(x_0, y_0)$ is the signal measured by the antenna measurement system at the same point:

$$EIRP = M_{\mathrm{EIRP}} \cdot \frac{P_{\mathrm{pr}}(x_0, y_0)}{b^2(x_0, y_0)} \cdot FF(K), \tag{1}$$

where $FF(K)$ is the probe-corrected far-field power pattern:

$$FF(K) = \left(\frac{4\pi}{\lambda^2}\right)^2 \cdot M \cdot \frac{|\delta_x \delta_y \sum_i b_i(p_i) \cdot \exp(-iK \cdot p_i)|^2}{G_{pr}(K)}, \tag{2}$$

where δ_x and δ_y are acquisition steps in X and Y axes, K is a direction in k-space where the pattern is calculated, b_i and p_i are amplitude and phase of the measured signal, and G_pr is far-field pattern of the probe. Here we assume that the gain of the probe is calibrated, but if it is not, it will be another source of uncertainty in the calculations.

We can estimate the errors in the following way:

- Mismatch factor - $\sigma_1 = 0.05\,\mathrm{dB}$, if all reflection coefficients are below $-11\,\mathrm{dB}$,

- Power measurement - σ_2 =0.15 dB for a spectrum analyzer (to get probe power, we also need to calibrate the RF path),
- RF path loss calibration - σ_3 =0.15 dB, defined by VNA accuracy,
- NF sample b_0 measurement - σ_4 =0.12 dB,
- FF pattern level - σ_5 =0.2 dB - considering that the probe gain is calibrated.

We see that the mismatch factor for well-matched measurement system and antennas doesn't introduce significant errors. For payloads without antenna test couplers and no direct LO access, phase errors caused by LO recovery methods can significantly increase the error in pattern values, turning it to the most important factor. Finally, a payload without any test access can suffer not only from increased FF errors, but also NF sample errors, as mentioned in Subsection **??**.

B. SFD

Saturating flux density is the value of the uplink flux density that will drive the downlink output into saturation. The power to the uplink probe is increased until the power at the downlink probe reaches saturation. Afterwards, SFD is calculated in a similar way to the EIRP, but here we need to measure the transmitted power to the uplink probe input P_{pr}. The same uncertainty considerations apply in this case:

$$SFD = \frac{(4\pi)}{\lambda^2} \cdot \frac{P_{\text{pr}}(x_0, y_0) \cdot b^2(x_0, y_0)}{M_{\text{SFD}}} \cdot FF(K). \quad (3)$$

C. Gain over Temperature, G/T

For G/T measurements, we need to measure power levels not only at the uplink probe input, but also at the downlink output (three times). Because of that, uncertainty of power measurements becomes the dominant source of uncertainty in G/T measurement:

$$\frac{G}{T} = kB \cdot \frac{1}{M_{G/T}} \cdot \frac{P_{\text{pr}}(x_0, y_0) \cdot b^2(x_0, y_0) \cdot \left(\frac{P_3 - P_2}{P_2 - P_1}\right)}{FF(K)}. \quad (4)$$

In the formula above, k is Boltzmann's constant, B is receiver bandwidth, $M_{G/T}$ is a mismatch factor, P_1 is noise level of the measurement system, P_2 is the noise of the DUT and the measurement system, and P_3 is the power measured when a CW signal with power of P_{pr} is transmitted from the uplink probe.

D. Gain Flatness, G/F

As for G/F, it combines error sources of both EIRP and SFD:

$$\frac{G}{F} = \frac{M_{SFD} \cdot M_{EIRP} \cdot FF(K_{up}) \cdot FF(K_{down})}{P_T(x_{01}, y_{01}) \cdot b^2(x_{01}, y_{01}) \cdot P_R(x_{02}, y_{02}) \cdot b^2(x_{02}, y_{02})}. \quad (5)$$

If an external mixer is used when LO is accessible, then this mixer must also be vector-calibrated and its calibration accuracy added to the error budget [8].

E. Uncertainty review

Table I provides the review of error budget that is possible to achieve with state-of-the-art measurement instruments and fully accessible payload (or with antenna test couplers available). A setup with no couplers and no direct LO access (XO output only) will have slightly higher uncertainties in far-field measurements, due to increased phase errors.

Param.	**Estimated terms of uncertainty**	**RSS,** $\pm dB$	**RSS (no access),** $\pm dB$
EIRP	$\sigma_{\text{EIRP}} = \sqrt{\sum_{i=1}^{5} \sigma_i^2}$	0.35	0.54
SFD	$\sigma_{\text{SFD}} = \sqrt{\sum_{i=1}^{5} \sigma_i^2}$	0.35	0.54
G/T	$\sigma_{G/T} = \sqrt{\sum_{i=1}^{5} \sigma_i^2 + 4\sigma_2^2}$	0.46	0.61
G/F	$\sigma_{G/F} = \sqrt{2\left(\sum_{i=1}^{5} \sigma_i^2\right)}$	0.5	0.76

TABLE I: Uncertainty total, accessible payload

For a fully integrated payload, however, the measured field and pattern will have even higher errors due to reflections and phase reconstruction errors. Estimating that the reflections will double the FF pattern and NF uncertainty, we will get the results shown in the last column of Table I.

IV. Conclusions

As it was shown, PNF measurements of the satellite payload are possible for any payload configurations, although the resulting accuracies (and the efforts to achieve them) are different. Several conclusions are important to underline:

- The largest common sources of uncertainties are power calibrations (path losses and probe gain) and absolute power measurements (power meter/spectrum analyzer).
- In a no-access (fully integrated) payload the stray signal path "static probe - moving probe - AUT" can be the most challenging error. Careful probe absorber positioning is required.
- As usual, the most important part of the NF measurement system is the phase coherency (and accuracy). Obtaining a reference signal can be one of the largest challenges, and having direct access to on-board LO source simplifies the measurement system and increases accuracy in case that antenna test couplers are not available.

In the end, the satellite system designer should take a decision which test points should be accessible, knowing how this choice impacts the accuracy of measurements and the cost of the measurement setup.

References

[1] T. M. Braun and W. R. Braun, *Satellite Communications Payload and System*. John Wiley & Sons, Ltd, 2021.

[2] S. Burgos, P. O. Iversen, T. Andersson, U. Wagner, T. Kozan, A. Jernberg, B. Priemer, M. Boumans, G. Pinchuk, R. Braun, and L. Shmidov, "Near-field hybrid test range from 400 MHz to 50 GHz in the ESTEC compact payload test range with RF upgrade for high frequencies," in *The 8th European Conference on Antennas and Propagation (EuCAP 2014)*, 2014, pp. 1075–1079.

[3] S. W. Schneider, J. Kemp, L. J. Foged, L. Scialacqua, F. Saccardi, M. Bandinelli, M. Bercigli, G. Guida, G. Giordanengo, F. Vipiana, M. Sabbadini, and G. Vecchi, "Satellite near-field testing and verification using physics-based interpolation technique and optimum sampling [AMTA corner]," *IEEE Antennas and Propagation Magazine*, vol. 55, no. 6, pp. 261–270, 2013.

[4] E. A. Barry, P. N. Betjes, D. J. Van Rensburg, and P. Pelland, "Implementation and validation of a satellite payload test suite for planar near field test ranges," in *2021 Antenna Measurement Techniques Association Symposium (AMTA)*, 2021, pp. 1–6.

[5] J. Hartmann, J. Habersack, and H.-J. Steiner, "Accurate and efficient satellite payload testing in compact ranges," in *28th ESA Antenna Workshop on Space Antenna Systems and Technologies*, 01 2005, p. 6.

[6] B. T. Walkenhorst and A. C. Newell, "Measuring G/T of active antennas using planar near-field scanners," in *2019 International Conference on Electromagnetics in Advanced Applications (ICEAA)*, 2019, pp. 0903–0908.

[7] P. Pelland, D. J. van Rensburg, and E. Barry, "Advances in characterizing complex frequency responses of frequency converting payloads in planar near-field test ranges," in *2019 13th European Conference on Antennas and Propagation (EuCAP)*, 2019, pp. 1–5.

[8] E. Barry, P. Betjes, P. Pelland, and D. J. van Rensburg, "Estimating uncertainties of system level RF parameters of transponder spacecraft payloads," in *2023 Antenna Measurement Techniques Association Symposium (AMTA)*, 2023, pp. 1–6.